

# Enhanced Bi-directional Motion Estimation for Video Frame Interpolation

Xin Jin<sup>1</sup> Longhai Wu<sup>1</sup> Guotao Shen<sup>1</sup> Youxin Chen<sup>1</sup> Jie Chen<sup>1</sup> Jayoon Koo<sup>2</sup> Cheul-hee Hahm<sup>2</sup>  
<sup>1</sup>Samsung Electronics (China) R&D Center <sup>2</sup>Samsung Electronics, South Korea  
{xin.jin, longhai.wu, guotao.shen, yx113.chen, ada.chen, j.goo, chhahm}@samsung.com

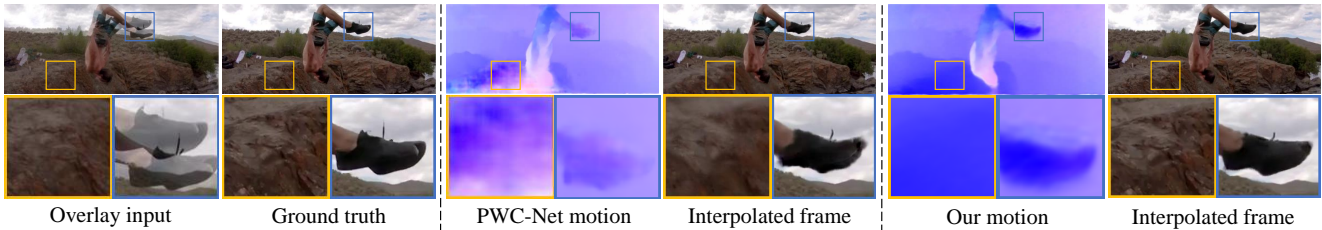


Figure 1. **First two columns:** Overlay inputs and ground truth intermediate frame. **Middle two columns:** Motion field (from first frame to second frame) by PWC-Net [33] and corresponding interpolated frame, where PWC-Net is end-to-end trained with our synthesis network. **Last two columns:** Motion field and interpolated frame by our motion model and synthesis network.

## Abstract

We present a novel simple yet effective algorithm for motion-based video frame interpolation. Existing motion-based interpolation methods typically rely on a pre-trained optical flow model or a U-Net based pyramid network for motion estimation, which either suffer from large model size or limited capacity in handling complex and large motion cases. In this work, by carefully integrating intermediate-oriented forward-warping, lightweight feature encoder, and correlation volume into a pyramid recurrent framework, we derive a compact model to simultaneously estimate the bi-directional motion between input frames. It is 15 times smaller in size than PWC-Net, yet enables more reliable and flexible handling of challenging motion cases. Based on estimated bi-directional motion, we forward-warp input frames and their context features to intermediate frame, and employ a synthesis network to estimate the intermediate frame from warped representations. Our method achieves excellent performance on a broad range of video frame interpolation benchmarks. Code will be available soon.

## 1. Introduction

Video frame interpolation aims to increase the frame rate of videos, by synthesizing non-existent intermediate frames between original successive frames. Increasing frame rate is not only beneficial for human perception [14], but also has wide applications including novel view synthesis [8], video compression [21] and adaptive streaming [35].

The key challenge for frame interpolation is the possible complex, large motions between input frames and intermediate frame. Based on whether a motion model is employed to capture the per-pixel motion (*i.e.*, optical flow) between frames, existing methods can be classified into two categories: motion-agnostic methods [26, 23, 5, 6], and motion-based methods [13, 19, 24, 3, 25, 27, 28]. With recent advances in optical flow [12, 10, 33, 34], motion-based interpolation has developed into a promising framework.

Motion-based interpolation involves two steps: (i) motion estimation, and (ii) frame synthesis. The estimated motion field is leveraged to guide the synthesis of intermediate frame by forward-warping [24, 25] or backward-warping [13, 28, 31] input frames towards the intermediate frame. Forward-warping is guided by motion from input frames to intermediate frame, while backward-warping requires motion in reversed direction. Although backward-warping has been traditionally used for frame synthesis, acquiring motion from *arbitrary* intermediate frame to input frames is often cumbersome, relying on specially-designed modules for approximation [13, 31]. Instead, motion from input frames to *arbitrary* intermediate frame can be easily approximated, solely by linearly scaling the bi-directional motion between input frames. Thus, forward-warping has emerged as a promising direction for frame interpolation [25].

Estimating bi-directional motion between input frames is a crucial step for all forward-warping based frame interpolation methods [24, 25] and many backward-warping based methods [13, 2, 31]. Existing methods typically rely on a pre-trained optical flow model [24, 25] or a U-Net based

pyramid network [31] for bi-directional motion. However, pre-trained optical flow models typically have large model size, and can hardly estimate extreme large motion beyond the training data. Recently, a U-Net based pyramid recurrent network is proposed for bi-directional motion [31]. It applies a U-Net as recurrent unit within a pyramid network, enabling customizable pyramid level to handle large motion. Nonetheless, U-Net has limited capacity in estimating complex motion, due to the lack of correlation volume, a vital ingredient in modern optical flow models [33, 34].

We present a novel simple but effective algorithm for forward-warping based frame interpolation. Our main contribution is a bi-directional motion estimator, which integrates intermediate-oriented forward-warping, lightweight feature encoder, and correlation volume into a pyramid recurrent framework. Compared to pre-trained optical flow models [33, 34], our method greatly reduces model size, and enables more flexible handling of large motion. Compared to existing pyramid recurrent motion estimators [37, 31], our design enhances the ability in handling complex motion, while further reducing the model size. Based on estimated bi-directional motion, we forward-warp input frames and their context features to the intermediate frame, and employ a simple synthesis network to predict the intermediate frame from warped representations. As shown in Figure 1, while our motion estimator is 15x smaller than PWC-Net [33], it can reliably handle complex and large motion, and enables better interpolation performance.

We conduct extensive experiments to verify the effectiveness of our interpolation method named EBME – **Enhanced Bi-directional Motion Estimation** for frame interpolation. Despite its small model size, EBME performs favorably against state-of-the-art methods on a broad range of benchmarks, from low resolution UCF101 [32], Vimeo90K [36], to moderate-resolution SNU-FILM [6] and extremely high-resolution 4K1000FPS [31].

## 2. Related Work

**General-purpose optical flow.** Optical flow, which measures per-pixel motion between successive frames, has witnessed great progress over the past few years [7, 12, 10, 33, 34]. Modern optical flow models follow similar design philosophy: extract CNN features for both input frames, construct a correlation volume (also called cost volume), and iteratively update flow field with correlation injected features. Correlation volume stores the similarity scores between the pixels of two images or CNN features, which is a more discriminative representation than CNN features for optical flow. Before constructing correlation volume, backward-warping is typically employed to align the second frame towards the first frame [33]. Warping aims to compensate for already estimated preliminary motion, which is beneficial for estimating large motion.

State-of-the-art optical flow models [33, 34] typically have a large number of parameters. Furthermore, when end-to-end trained with a synthesis network for frame interpolation, they are prone to overfit the motion magnitude of training data. Our bi-directional motion estimator borrows some designs from state-of-the-art optical flow models, but is much more lightweight, and can flexibly handle large motion cases beyond the training data (see Figure 1).

**Bi-directional motion estimation.** General-purpose optical flow models typically estimate single-directional motion between input frames. However, forward-warping based interpolation methods require bi-directional motion [24, 25]. Even backward-warping based methods may also rely on bi-directional motion to approximate the motion from intermediate frame to input frames [2, 31]. Running a pre-trained optical flow model twice can obtain bi-directional motion, but leads to doubled computational cost.

U-Net [30] provides a powerful framework for dense prediction tasks, and has been employed to simultaneously estimate bi-directional motion for frame interpolation [13]. Recently, U-Net based pyramid recurrent network is exploited to estimate possible extremely large bi-directional motion [31]. Nonetheless, U-Net is over-simplified for motion estimation, due to the lack of correlation based features. By contrast, our model estimates bi-directional motion from correlation injected features.

**Intermediate-oriented warping.** Forward-warping or backward-warping input frames to intermediate frame is a common step before frame synthesis for motion-based interpolation. In addition, intermediate-oriented backward-warping has also been adopted to directly estimate the motion from intermediate frame to input frames [37, 9].

While for bi-directional motion estimation, it might seem counter-intuitive to perform intermediate-oriented warping, since the target is not the motion from input frames to certain *intermediate* frame. Actually, in [31], backward-warping is adopted to align the features of input frames towards each other for bi-directional motion estimation.

We argue that for bi-directional motion estimation, intermediate-oriented forward-warping is a better option than forward-warping or backward-warping that align one input frame towards another. In case of inaccurate initial bi-directional motion, warping one input frame to another might create serious misalignment, but intermediate-oriented forward-warping based on scaled motion can linearly reduce the possible motion errors. We empirically show the immense advantage of intermediate-oriented forward-warping for bi-directional motion estimation.

**Pyramid recurrent motion estimator.** Many of modern optical flow models is built upon a pyramid structure to es-

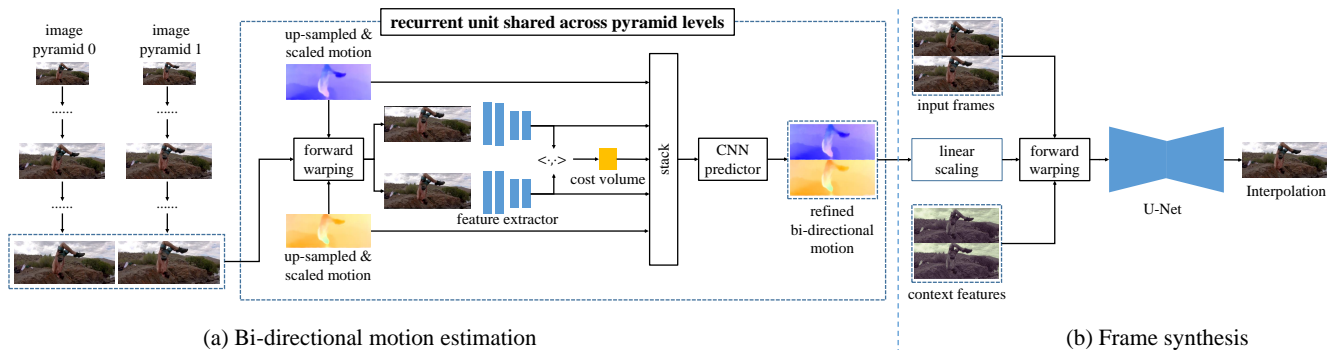


Figure 2. Overview of our frame interpolation algorithm. **(a)** We repeatedly apply a novel compact recurrent unit across image pyramids to estimate the bi-directional motion between input frames, where the recurrent unit is integrated with intermediate-oriented forward-warping, lightweight feature encoder, and correlation volume (*i.e.*, cost volume). **(b)** Based on estimated bi-directional motion, we forward-warp input frames and their context features, and employ a U-Net as synthesis network to predict the intermediate frame.

estimate optical flow from coarse-to-fine [33, 11]. Recently, Sim *et al.* [31] employ a U-Net as recurrent unit, and repeatedly apply it within a pyramid network to estimate the bi-directional motion. The recurrent design not only reduces parameter, but also allows to use a larger number of pyramid levels in testing to handle extremely motion cases beyond the training phase. Instead of using a simple U-Net, we design a compact recurrent unit integrated with intermediate-oriented forward-warping and correlation volume.

Lee *et al.* [16] proposed a single-directional motion estimator within a pyramid recurrent framework. It directly determines the motion by peak correlation values, and needs to run twice to obtain bi-directional motion.

**Forward-warping for frame synthesis.** In literature, forward-warping is less adopted than backward-warping for frame synthesis. This is probably because forward-warping may lead to holes in the warped output. Niklaus and Liu [24] demonstrated that this issue may be remedied by warping both input frames, since the holes in one warped frame can be naturally filled by the context information from another warped frame. Another limitation of forward-warping is that multiple pixels in source image may be mapped to the same target location. To solve this issue, Niklaus and Liu [25] developed a softmax splatting operation to adaptively assign weights to conflicted pixels.

Building upon recent advances of forward-warping, we employ forward-warping for both motion estimation and frame synthesis. In particular, we use the average splatting operation in [25] as forward-warping, rather than the more complicated softmax splatting. It directly averages the conflicted pixels to generate the pixel in target position.

### 3. Our Approach

Figure 2 gives an overview of our frame interpolation algorithm, where we first estimate the bi-directional motion

between input frames, and then employ a synthesis network to predict the intermediate frame.

#### 3.1. Bi-directional Motion Estimation

**Macro pyramid recurrent network.** As shown in Figure 2 (a), the macro structure of our bi-directional motion estimator is a pyramid recurrent network. Given two input frames, we firstly construct image pyramids for them, then repeatedly apply a novel recurrent unit across the pyramid levels to estimate the bi-directional motion from coarse-to-fine. This macro design is parameter-efficient, and enables customized pyramid level in testing. Our main innovation is the recurrent unit repeatedly applied on the pyramids.

**Basic structure of recurrent unit.** We design a compact bi-directional motion estimator as our recurrent unit. At each pyramid level, we first up-sample the estimated bi-directional motion from previous level as initial motion, then forward-warp the input frames to a hidden intermediate frame based on scaled initial motion. For the top pyramid level, the initial motion is set to zero. Given warped frames, we employ a lightweight feature encoder to extract CNN features for them, then construct partial correlation volume with CNN features, and feed correlation injected features to a CNN predictor to estimate the bi-directional motion.

Below, we describe the key components involved in our recurrent unit separately, including intermediate-oriented forward-warping, lightweight feature encoder, and correlation based motion estimation.

**Intermediate-oriented forward-warping.** At each pyramid level, we firstly forward-warp both input frames towards a hidden intermediate frame to align their pixels. As aforementioned, while backward-warping has been employed to align the two input frames towards each other for bi-directional motion estimation [31], it may lead to serious

misalignment in case of inaccurate initial bi-directional motion. By contrast, intermediate-oriented forward-warping based on scaled motion has the chance to linearly reduce the possible motion errors.

Formally, at the  $i$ th pyramid level, given two input frames  $I_0^i$  and  $I_1^i$ , let  $\hat{F}_{0 \rightarrow 1}^i$  and  $\hat{F}_{1 \rightarrow 0}^i$  denote *initial* bi-directional motion, which is up-sampled from previous level. Let  $t \in (0, 1)$  denote the intermediate temporal position, then intermediate-oriented motion  $\hat{F}_{0 \rightarrow t}^i$  and  $\hat{F}_{1 \rightarrow t}^i$  can be easily obtained by linear scaling the initial motion, *i.e.*,  $\hat{F}_{0 \rightarrow t}^i = t \cdot \hat{F}_{0 \rightarrow 1}^i$ , and  $\hat{F}_{1 \rightarrow t}^i = (1 - t) \cdot \hat{F}_{1 \rightarrow 0}^i$ . We note that the temporal position  $t$  here does not need to be equal to the temporal position of the target intermediate frame to be interpolated. We fix  $t$  as 0.5 for simplicity. With  $\hat{F}_{0 \rightarrow 0.5}^i$  and  $\hat{F}_{1 \rightarrow 0.5}^i$ , we forward-warp  $I_0^i$  and  $I_1^i$  to align their pixels on the latent middle frame  $I_{0.5}^i$ .

**Lightweight feature encoder.** Pyramidal optical flow models like PWC-Net [33] typically require a feature encoder with many down-sampling layers to construct feature pyramid. To handle large motion, PWC-Net employ a feature encoder of 6 down-sampling layers.

Benefiting from our outer image pyramid that handles large motion with customizable pyramid level, the feature encoder of our recurrent unit does not need many down-sampling layers. We employ an extremely lightweight feature encoder to extract CNN features for both warped frames. It has two convolutional stages, 3 layers for the first stage, and 6 layers for the second stage. Our feature encoder has only about 0.1 M parameters. By contrast, PWC-Net’s feature encoder has 1.7M parameters.

**Correlation based motion estimation.** With extracted CNN features for both warped frames, we construct a partial cost volume, and set the local search range on the feature map of the second frame as 4. Then, we use a 6-layer convolutional network to simultaneously predict the bi-directional motion. Its input is the concatenation of CNN features for both warped frames, cost volume, and up-sampled bi-directional motion. Since our feature encoder has two down-sampling layers, the estimated motion is at 1/4 resolution of the input frame. We use bi-linear interpolation to up-sample the motion vector to original resolution.

**Customized pyramid level in testing.** We main encounter extreme large motion cases in testing beyond the training phase. Based on the pyramid recurrent framework, a simple solution is to use more pyramid levels in testing when necessary. While previous works [37, 31] determine the pyramid level by experiments, we suggest a simple calculation method, and verify it by experiments.

Assume that we use a  $L^{train}$  level pyramid for training, and the averaged width (or height) of test images is  $n$  times

of the training images. Then, we can calculate a proper test pyramid level by  $L^{test} = \text{ceil}(L^{train} + \log_2 n)$ , where  $\text{ceil}()$  rounds up a float number to get an integer.

For our training Vimeo90K dataset, the resolution is  $448 \times 256$ , and we use a 3-level pyramid for training. For our benchmark datasets SNU-FILM [6] and 4K1000FPS [31], most images in SNU-FILM is about 720p, and 4K1000FPS has a resolution of 4K. Based on our suggested calculation method, we set the test pyramid level for SNU-FILM and 4K1000FPS as 5 and 7, respectively.

### 3.2. Frame Synthesis

Given estimated bi-directional motion, we firstly linearly scale it to obtain the motion from input frames to intermediate frame, then forward-warp input frames and their context features, and employ a synthesis network to predict the intermediate frame from warped representations.

**A simple baseline synthesis network.** The design of our synthesis network follows previous context-aware synthesis networks [25, 9], which takes both warped frames and warped context features as input. We extract 4-level pyramid context features for both input frames.

We employ a simple U-Net as our synthesis network, which has four down-sampling layers in the encoder part, and four up-sampling layers in the decoder part. The synthesis network takes warped frames, warped context features, original images, and bi-directional motion as input, and outputs a mask  $M$  for combining the warped frames, and a residual image  $\Delta I_t$  for further refinement. We refer to this synthesis network as our *base* synthesis network.

Formally, given input frames  $I_0$  and  $I_1$ , estimated motion from input frames to intermediate frame  $F_{0 \rightarrow t}$  and  $F_{1 \rightarrow t}$ , the interpolated frame  $\hat{I}_t$  is obtained by:

$$I_t = M \odot \vec{\mathcal{W}}(I_0, F_{0 \rightarrow t}) + (1 - M) \odot \vec{\mathcal{W}}(I_1, F_{1 \rightarrow t}) + \Delta I_t \quad (1)$$

where  $\odot$  denotes element-wise multiplication,  $\vec{\mathcal{W}}$  denotes the forward-warping operation. We note that when training on Vimeo90K [36], we set  $t = 0.5$ , but for testing, we can set  $t$  to arbitrary value in  $(0, 1)$ .

**High-resolution synthesis with convex down-sampling.** Higher resolution input has advantages for dense prediction tasks [29, 18]. We verify this for frame synthesis. Specifically, if we up-sample the input frames and estimated bi-directional motion to 2x resolution, and feed them to our synthesis network, we will obtain an interpolated frame with 2x resolution. Then, we can recover it to original resolution using bi-linear based down-sampling.

We design a convex down-sampling strategy, which achieves better performance than bi-linear down-sampling

(0.1 dB improvement on the “extreme” subset of SNU-FILM [6]), by fusing more pixels during down-sampling. Specifically, we add a lightweight head to our synthesis network to predict  $5 \times 5$  dynamic filters for the pixels with stride 2 on interpolated high-resolution frame. These filters allow us to take a convex weighted combination over the  $5 \times 5$  neighborhoods of the interpolated high-resolution frame to predict each pixel of the target frame. We refer to this structure as *high-resolution* synthesis network.

### 3.3. Architecture Variants

We name our frame interpolation method as EBME – Enhanced Bi-directional Motion Estimation for frame interpolation. We construct three versions of EBME, with almost the same model size but increased computational cost:

- **EBME:** It combines our bi-directional motion estimator with the base version of synthesis network.
- **EBME-H:** It combines our motion estimator with the high-resolution version of synthesis network.
- **EBME-H\*:** It uses the test-time augmentation (refer to Section 3.4) with EBME-H, which doubles the computational cost but further improves performance.

### 3.4. Implementation Details

**Loss function.** We train our model only with the synthesis loss, without auxiliary supervision for motion. Our loss is weighted sum of Charbonnier loss [4] and census loss [22] between ground truth  $I_t^{GT}$  and our interpolation  $I_t$ :

$$L = \rho(I_t^{GT} - I_t) + \lambda \cdot L_{cen}(I_t^{GT}, I_t), \quad (2)$$

where  $\rho(x) = (x^2 + \epsilon^2)^\alpha$  is the Charbonnier function,  $L_{cen}$  is the census loss, and  $\lambda$  is a trade-off hyper-parameter. We use  $\alpha = 0.5$  and  $\epsilon = 10^{-6}$  for Charbonnier loss, and empirically set  $\lambda = 0.1$ .

**Training dataset.** We train our model on the Vimeo90K dataset [36], which contains 51,312 triplets with resolution of  $448 \times 256$  for training. We augment the training images by randomly cropping  $256 \times 256$  patches. We also apply random flipping, rotating, reversing the order of the triplets for data augmentation.

**Optimization.** Our optimizer is AdamW [20] with weight decay  $10^{-4}$  for 0.8 M iterations, using a batch size of 32. We gradually reduce the learning rate during training from  $2 \times 10^{-4}$  to  $2 \times 10^{-5}$  using cosine annealing.

**Test-time augmentation.** We verify a practice strategy described in [9]. We flip the input frames horizontally and vertically to get augmented test data, and use our model to infer two results and reverse the flipping. A more robust prediction can be obtained by averaging above two results.

## 4. Experiments

### 4.1. Experiment Settings

**Evaluation datasets.** While our method is trained only on Vimeo90K [36], we evaluate it on a broad range of benchmarks with different resolutions.

- **UCF101 [32]:** The test set of UCF101 contains 379 triplets with a resolution of  $256 \times 256$ . UCF101 contains a large variety of human actions.
- **Vimeo90K [36]:** The test set of Vimeo90K contains 3,782 triplets with a resolution of  $448 \times 256$ .
- **SNU-FILM [6]:** This dataset contains 1,240 triplets, and most of them are of the resolution around  $1280 \times 720$ . It contains four subsets with increasing motion scales – easy, medium, hard, and extreme.
- **4K1000FPS [31]:** This is a 4K resolution benchmark that enables multi-frame ( $\times 8$ ) interpolation.

**Metrics.** We calculate the peak signal-to-noise ratio (PSNR) and structure similarity (SSIM) for the quantitative evaluation of interpolation accuracy. For the running time, we follow the practice of [28], and test all models with a RTX 2080 Ti GPU for interpolating the intermediate frame of the “Urban” sequence in Middle-bury benchmark [1], which has a resolution of  $640 \times 480$ .

### 4.2. Comparisons with State-of-the-art Methods

We compare with state-of-the-art methods, including CyclicGen [17], DAIN [2], CAIN [6], SoftSplat [25], AdaCoF [15], BMBC [27], ABME [28], and XVFI [31]. We report their results by executing the source code and trained models. For SoftSplat which has not released the model, we copy the results from the original paper.

**Low and moderate resolution frame interpolation.** Table 1 reports the comparison results on low-resolution UCF101 and Vimeo90K datasets. As UCF101 has similar resolution with Vimeo90K, we set the test pyramid level as 3. Our EBME-H\* achieves best performance on both benchmarks. Our EBME also outperforms many state-of-the-art models including CyclicGen, DAIN, CAIN, AdaCoF, BMBC, and XVFI.

Table 1 also reports the comparison results on SNU-FILM. Our EBME-H and EBME-H\* perform similar with ABME [28] on the “hard” and “extreme” subsets, but have better performance on the “easy” and “medium” subsets. It is worth noting that our models are about 4.5x smaller than ABME, and run much faster.

Figure 3 gives two examples from the “extreme” subset from SNU-FILM. Our methods produce better interpolation results than ABME for some detailed textures (first



methods	UCF101	Vimeo90K	SNU-FILM				parameters (millions)	runtime (seconds)
			easy	medium	hard	extreme		
CyclicGen [17]	35.11/0.968	32.09/0.949	37.72/0.984	32.47/0.955	26.95/0.887	22.70/0.808	19.8	0.09
DAIN [2]	34.99/0.968	34.71/0.976	39.73/ <b>0.990</b>	35.46/0.978	30.17/0.934	25.09/0.858	24.0	0.13
CAIN [6]	34.91/ <b>0.969</b>	34.65/0.973	39.89/ <b>0.990</b>	35.61/0.978	29.90/0.929	24.78/0.851	42.8	0.04
SoftSplat [25]	<b>35.39/0.952</b>	36.10/0.970	-	-	-	-	-	-
AdaCoF [15]	34.90/0.968	34.47/0.973	39.80/ <b>0.990</b>	35.05/0.975	29.46/0.924	24.31/0.844	22.9	<b>0.03</b>
BMBC [27]	35.15/ <b>0.969</b>	35.01/0.976	39.90/ <b>0.990</b>	35.31/0.977	29.33/0.927	23.92/0.843	11.0	0.77
ABME [28]	35.38/ <b>0.970</b>	<b>36.18/0.981</b>	39.59/ <b>0.990</b>	35.77/ <b>0.979</b>	<b>30.58/0.936</b>	<b>25.42/0.864</b>	18.1	0.22
XVFI <sub>v</sub> [31]	35.18/0.952	35.07/0.976	39.92/0.985	35.37/0.965	29.58/0.861	24.17/0.769	<b>5.5</b>	0.04
EBME (ours)	35.30/ <b>0.969</b>	35.58/0.978	40.01/ <b>0.991</b>	35.80/ <b>0.979</b>	30.42/0.935	25.25/0.861	<b>3.9</b>	<b>0.02</b>
EBME-H (ours)	35.35/ <b>0.969</b>	36.06/ <b>0.980</b>	<b>40.20/0.991</b>	<b>36.00/0.980</b>	30.54/ <b>0.936</b>	25.30/0.862	<b>3.9</b>	0.04
EBME-H* (ours)	<b>35.41/0.970</b>	<b>36.19/0.981</b>	<b>40.28/0.991</b>	<b>36.07/0.980</b>	<b>30.64/0.937</b>	<b>25.40/0.863</b>	<b>3.9</b>	0.08

Table 1. Qualitative (PSNR/SSIM) comparisons to state-of-the-art methods on UCF101 [32], Vimeo90K [36] and SNU-FILM [6] benchmarks. **RED**: best performance, **BLUE**: second best performance.



Figure 3. Visual comparisons on two examples from the “extreme” subset of SNU-FILM [6]. The first two rows show the synthesis results for detailed textures, while the last two rows demonstrate the results with complex and large motion.

two rows), and give promising results for large motion cases (last two rows), much better than CAIN and AdaCoF, and slightly better than ABME.

**4K resolution multiple frame interpolation.** Table 2 reports the 8x interpolation results on 4K1000FPS. Our method achieves the best performance by SSIM, and slight inferior results by PSNR. Furthermore, our method naturally supports arbitrary-time frame interpolation, and can fully re-use the estimated bi-directional motion by linear scaling when interpolating multiple intermediate frames at different time positions. By contrast, while XVFI [31] can reuse the bi-directional motion, it must estimate the intermediate flow for backward-warping with an extra network at each time position.

Figure 4 shows two interpolation examples. Our methods give better performance for small moving objects. The U-Net based motion estimator in XVFI might have difficulty in capturing the motion of extreme small objects.

**Parameter and inference efficiency.** As shown the last two columns in Table 1, our frame interpolation algorithm has much less parameters than state-of-the-art methods and runs very fast. In particular, due to the macro recurrent design and the lightweight feature encoder, our bi-directional motion estimator only has about 0.6 M parameters.

### 4.3. Analysis of Our Motion Estimator

We present analysis of our motion estimator on the “easy” and “extreme” subsets of SNU-FILM [6], which

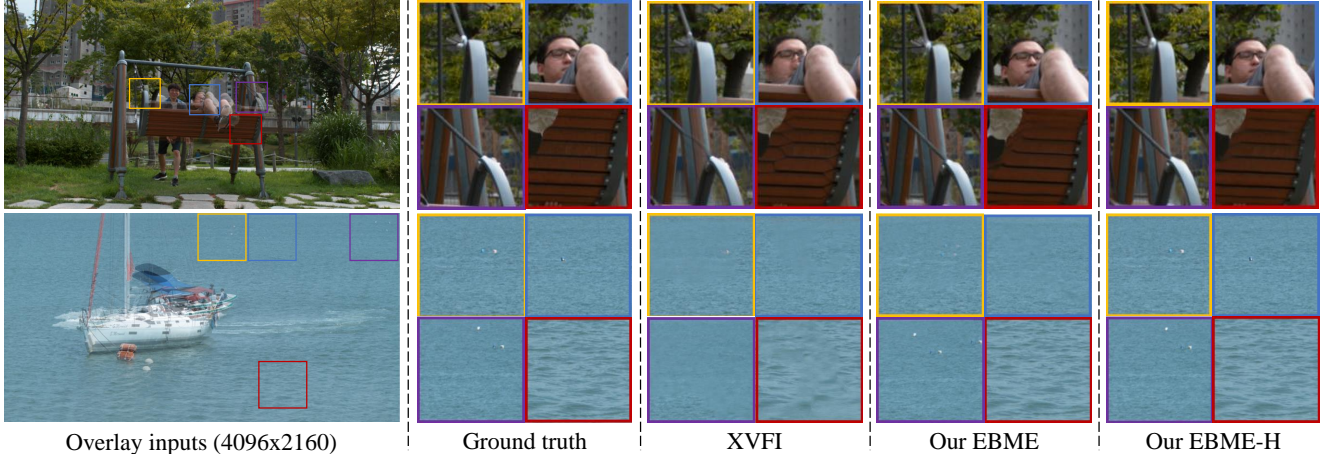


Figure 4. Visual comparisons on 4K1000FPS [31]. XVFI [31] tends to miss the moving small objects, while our EBME-H gives interpolation results close to the ground truth.

methods	arbitrary	reuse flow	4K1000FPS	
			PSNR	SSIM
DAIN [2]	✓	partial	26.78	0.807
AdaCoF [15]	×	×	23.90	0.727
ABME [28]	✓	×	<b>30.16</b>	0.879
XVFI [31]	✓	partial	<u>30.12</u>	0.870
EBME (ours)	✓	✓	27.86	0.881
EBME-H (ours)	✓	✓	28.72	<u>0.889</u>
EBME-H* (ours)	✓	✓	29.46	<b>0.902</b>

Table 2. Comparisons on 4K1000FPS [36] for 8x interpolation. **RED**: best performance, **BLUE**: second best performance.

mainly contain small and large motion, respectively.

**Design Choices of Motion Estimator.** In Table 3, we report the ablation results for the design choices of our bi-directional motion estimator.

- **Warping type:** We use scaled bi-directional motion to forward-warp both input frames to the intermediate frame. Despite being a minor difference, our intermediate-oriented forward-warping (denoted as “inter-forward”) shows immense advantages for bi-directional motion estimation, when compared with forward-warping and backward-warping that align input frames towards each other.
- **Feature encoder:** We investigate three settings for our feature encoder one convolutional stage of 9 layers; two-stage with 3 layers for the first stage, and 6 layers for the second stage; three-stage with 3 layers for each of the stage. We double the number of filters with down-sampling layers. More down-sampling layers are beneficial for large motion but may lead to rough estimate on the whole. We find that two-stage achieves

experiments	methods	SNU-FILM (PSNR $\uparrow$ )	
		easy	extreme
warping type	forward	38.27	21.68
	<b>inter-forward</b>	40.01	25.25
	backward	34.38	22.27
feature encoder	1-stage	39.98	25.20
	<b>2-stage</b>	40.01	25.25
	3-stage	39.98	25.15
correlation	without	39.98	25.19
	<b>with</b>	40.01	25.25
test pyramid	3-level	40.03	24.80
	4-level	40.01	25.20
	<b>5-level</b>	40.01	25.25
	6-level	40.01	25.22

Table 3. Impacts of the design choices of our bi-directional motion estimator, integrated with base synthesis network for frame interpolation. Default settings are marked in **gray**.

the best trade-off.

- **Correlation volume:** Removing correlation volume from our motion model leads to slightly inferior quantitative results. However, as shown in Figure 5, without a correlation volume, our estimator may have difficulty in estimating complex motion, and lead to artifacts in local regions. Although these local artifacts might have little impact on evaluation metric, they may have bad affects for human perception.
- **Test pyramid level:** A 5-level image pyramid achieves good performance on the “extreme” subset. Further increasing pyramid level does not lead to better results. This is consistent with our suggested calculation method described in Section 3.1.

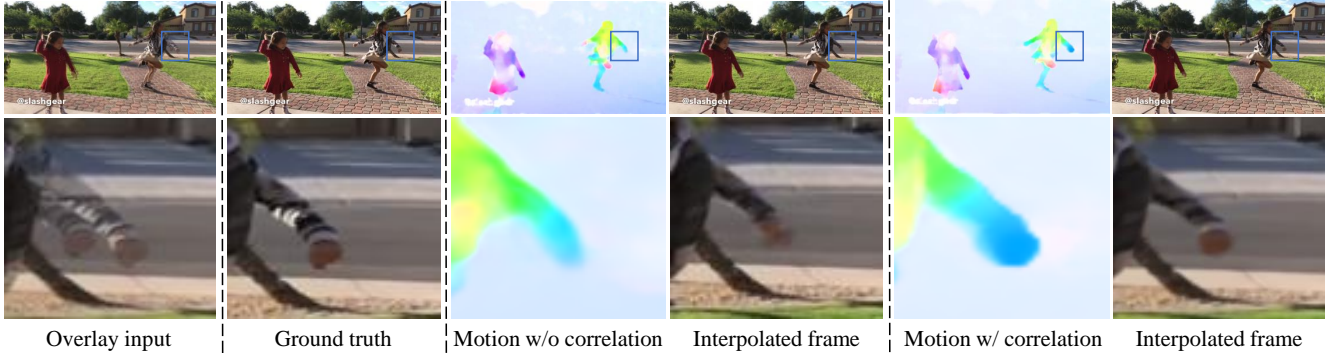


Figure 5. Visual comparisons between the results without and with a correlation volume. **Middle two columns**: results without a correlation volume. **Right two columns**: results with a correlation volume. Without a correlation volume, our estimator may fail to capture the complex nonlinear motion, and lead to artifacts on interpolated frame.

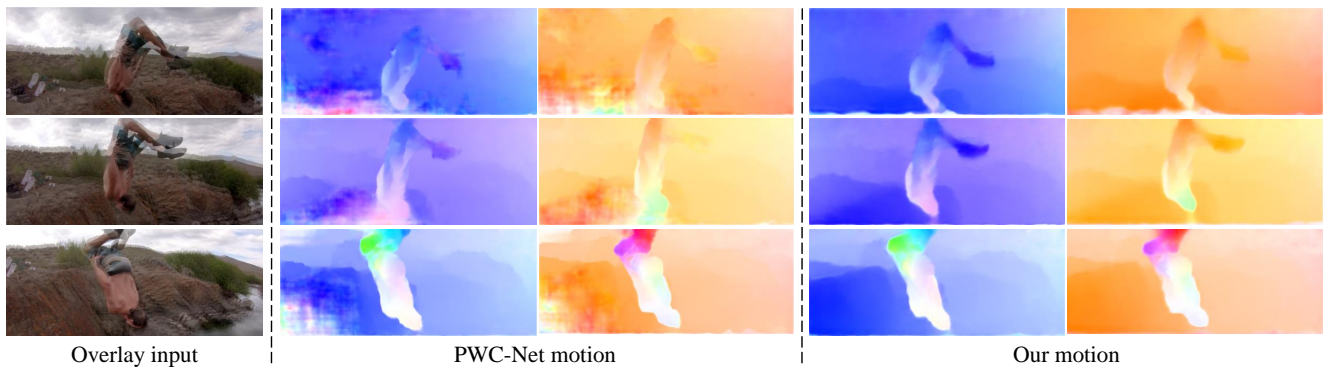


Figure 6. Visual comparison between of estimated bi-directional motion by PWC-Net [33] and our motion estimator. Both motion models are end-to-end trained from scratch with our base version of synthesis network.

experiments	methods	SNU-FILM (PSNR $\uparrow$ )		param. (M)
		easy	extreme	
warp approx.	PWC (fix)	35.98	23.09	9.4
	PWC (ft)	37.81	<u>23.81</u>	9.4
	PWC (rand)	<u>37.86</u>	23.59	9.4
	RAFT (rand)	37.29	23.21	<u>5.3</u>
	ours (rand)	<b>37.88</b>	<b>24.00</b>	<b>0.6</b>
full pipeline	PWC (fix)	39.65	<u>25.08</u>	12.7
	PWC (ft)	<b>40.04</b>	24.80	12.7
	PWC (rand)	<u>40.03</u>	24.53	12.7
	RAFT (rand)	39.98	24.69	<u>8.6</u>
	ours (rand)	40.01	<b>25.25</b>	<b>3.9</b>

Table 4. Comparisons of motion quality between our model, PWC-Net [33] and RAFT [34]. **RED**: best performance, **BLUE**: second best performance.

**Motion Quality Analysis.** We quantitatively compare our motion quality with PWC-Net [33] and RAFT [34] from two aspects: interpolation by averaging two warped frames, and interpolation by our full pipeline. As shown in Table 4, despite its small model size, our motion estimator consistently achieves the best results on “extreme” subset. Figure 6 shows visual examples, where our model gives more

smooth and accurate estimation for challenging motion.

We also have a meaningful observation with PWC-Net. With our full pipeline, fixing pre-trained PWC-Net (marked with “fix”) leads to inferior performance on the “easy” subset than the fine-tuned version (marked with “ft”) and randomly initialized version (marked with “rand”). But, it has better performance on the “extreme” subset. This verifies that end-to-end training with the synthesis network makes an optical flow model to fit the motion distribution on the training data, leading to inferior results with large motion.

## 5. Conclusion

This work presented a lightweight yet effective frame interpolation algorithm, based on a novel bi-directional motion estimator. Despite its small size, our method achieved excellent performance on a wide range of benchmarks. We expect that our design choices for bi-directional motion estimation can also be applied for designing lightweight general-purpose optical flow models.



## References

- [1] Simon Baker, Daniel Scharstein, JP Lewis, Stefan Roth, Michael J Black, and Richard Szeliski. A database and evaluation methodology for optical flow. *IJCV*, 2011.
- [2] Wenbo Bao, Wei-Sheng Lai, Chao Ma, Xiaoyun Zhang, Zhiyong Gao, and Ming-Hsuan Yang. Depth-aware video frame interpolation. In *CVPR*, 2019.
- [3] Wenbo Bao, Wei-Sheng Lai, Xiaoyun Zhang, Zhiyong Gao, and Ming-Hsuan Yang. MEMC-Net: Motion estimation and motion compensation driven neural network for video interpolation and enhancement. *TPAMI*, 2019.
- [4] Pierre Charbonnier, Laure Blanc-Feraud, Gilles Aubert, and Michel Barlaud. Two deterministic half-quadratic regularization algorithms for computed imaging. In *ICIP*, 1994.
- [5] Xianhang Cheng and Zhenzhong Chen. Video frame interpolation via deformable separable convolution. In *AAAI*, 2020.
- [6] Myungsub Choi, Heewon Kim, Bohyung Han, Ning Xu, and Kyoung Mu Lee. Channel attention is all you need for video frame interpolation. In *AAAI*, 2020.
- [7] Alexey Dosovitskiy, Philipp Fischer, Eddy Ilg, Philip Hausser, Caner Hazirbas, Vladimir Golkov, Patrick Van Der Smagt, Daniel Cremers, and Thomas Brox. FlowNet: Learning optical flow with convolutional networks. In *ICCV*, 2015.
- [8] John Flynn, Ivan Neulander, James Philbin, and Noah Snavely. Deepstereo: Learning to predict new views from the world’s imagery. In *CVPR*, 2016.
- [9] Zhewei Huang, Tianyuan Zhang, Wen Heng, Boxin Shi, and Shuchang Zhou. RIFE: Real-time intermediate flow estimation for video frame interpolation. *arXiv preprint arXiv:2011.06294*, 2020.
- [10] Tak-Wai Hui, Xiaoou Tang, and Chen Change Loy. Lite-FlowNet: A lightweight convolutional neural network for optical flow estimation. In *CVPR*, 2018.
- [11] Junhwa Hur and Stefan Roth. Iterative residual refinement for joint optical flow and occlusion estimation. In *CVPR*, 2019.
- [12] Eddy Ilg, Nikolaus Mayer, Tonmoy Saikia, Margret Keuper, Alexey Dosovitskiy, and Thomas Brox. FlowNet 2.0: Evolution of optical flow estimation with deep networks. In *CVPR*, 2017.
- [13] Huaizu Jiang, Deqing Sun, Varun Jampani, Ming-Hsuan Yang, Erik Learned-Miller, and Jan Kautz. Super slomo: High quality estimation of multiple intermediate frames for video interpolation. In *ICCV*, 2018.
- [14] Yoshihiko Kuroki, Haruo Takahashi, Masahiro Kusakabe, and Ken-ichi Yamakoshi. Effects of motion image stimuli with normal and high frame rates on EEG power spectra: comparison with continuous motion image stimuli. *Journal of the Society for Information Display*, 2014.
- [15] Hyeongmin Lee, Taeoh Kim, Tae-young Chung, Daehyun Pak, Yuseok Ban, and Sangyoun Lee. AdaCoF: Adaptive collaboration of flows for video frame interpolation. In *CVPR*, 2020.
- [16] Sungho Lee, Narae Choi, and Woong Il Choi. Enhanced correlation matching based video frame interpolation. In *WACV*, 2022.
- [17] Yu-Lun Liu, Yi-Tung Liao, Yen-Yu Lin, and Yung-Yu Chuang. Deep video frame interpolation using cyclic frame generation. In *AAAI*, 2019.
- [18] Ze Liu, Han Hu, Yutong Lin, Zhuliang Yao, Zhenda Xie, Yixuan Wei, Jia Ning, Yue Cao, Zheng Zhang, Li Dong, et al. Swin transformer v2: Scaling up capacity and resolution. *arXiv preprint arXiv:2111.09883*, 2021.
- [19] Ziwei Liu, Raymond A Yeh, Xiaoou Tang, Yiming Liu, and Aseem Agarwala. Video frame synthesis using deep voxel flow. In *ICCV*, 2017.
- [20] Ilya Loshchilov and Frank Hutter. Decoupled weight decay regularization. *arXiv preprint arXiv:1711.05101*, 2017.
- [21] Guo Lu, Xiaoyun Zhang, Li Chen, and Zhiyong Gao. Novel integration of frame rate up conversion and HEVC coding based on rate-distortion optimization. *TIP*, 2017.
- [22] Simon Meister, Junhwa Hur, and Stefan Roth. Unflow: Unsupervised learning of optical flow with a bidirectional census loss. In *AAAI*, 2018.
- [23] Simone Meyer, Abdelaziz Djelouah, Brian McWilliams, Alexander Sorkine-Hornung, Markus Gross, and Christopher Schroers. Phasenet for video frame interpolation. In *CVPR*, 2018.
- [24] Simon Niklaus and Feng Liu. Context-aware synthesis for video frame interpolation. In *CVPR*, 2018.
- [25] Simon Niklaus and Feng Liu. Softmax splatting for video frame interpolation. In *CVPR*, 2020.
- [26] Simon Niklaus, Long Mai, and Feng Liu. Video frame interpolation via adaptive separable convolution. In *ICCV*, 2017.
- [27] Junheum Park, Keunsoo Ko, Chul Lee, and Chang-Su Kim. BMBC: Bilateral motion estimation with bilateral cost volume for video interpolation. In *ECCV*, 2020.
- [28] Junheum Park, Chul Lee, and Chang-Su Kim. Asymmetric bilateral motion estimation for video frame interpolation. In *ICCV*, 2021.
- [29] Joseph Redmon and Ali Farhadi. Yolov3: An incremental improvement. *arXiv preprint arXiv:1804.02767*, 2018.
- [30] Olaf Ronneberger, Philipp Fischer, and Thomas Brox. U-Net: Convolutional networks for biomedical image segmentation. In *International Conference on Medical image computing and computer-assisted intervention*, 2015.
- [31] Hyeonjun Sim, Jihyong Oh, and Munchurl Kim. XVFI: Extreme video frame interpolation. In *ICCV*, 2021.
- [32] Khurram Soomro, Amir Roshan Zamir, and Mubarak Shah. UCF101: A dataset of 101 human actions classes from videos in the wild. *arXiv preprint arXiv:1212.0402*, 2012.
- [33] Deqing Sun, Xiaodong Yang, Ming-Yu Liu, and Jan Kautz. PWC-Net: CNNs for optical flow using pyramid, warping, and cost volume. In *CVPR*, 2018.
- [34] Zachary Teed and Jia Deng. RAFT: Recurrent all-pairs field transforms for optical flow. In *ECCV*, 2020.
- [35] Jiyan Wu, Chau Yuen, Ngai-Man Cheung, Junliang Chen, and Chang Wen Chen. Modeling and optimization of high frame rate video transmission over wireless networks. *IEEE Transactions on Wireless Communications*, 2015.
- [36] Tianfan Xue, Baian Chen, Jiajun Wu, Donglai Wei, and William T Freeman. Video enhancement with task-oriented flow. *IJCV*, 2019.

- [37] Haoxian Zhang, Yang Zhao, and Ronggang Wang. A flexible recurrent residual pyramid network for video frame interpolation. In *ECCV*, 2020.